Rock and Soil Mechanics

Volume 41 | Issue 4 Article 3

9-27-2020

Evolution law of pore-size distribution in soil-water retention test

Geng NIU
State Key Laboratory of Structural Analysis of Industrial Equipment, Department of Engineering Mechanics, Dalian University of Technology, Dalian, Liaoning 116085, China

Long-tan SHAO
State Key Laboratory of Structural Analysis of Industrial Equipment, Department of Engineering Mechanics, Dalian University of Technology, Dalian, Liaoning 116085, China

De-an SUN
Shandong Province Administration of Haihe River Basin, Jinan, Shandong 250100, China

Chang-fu WEI
Shandong Province Administration of Haihe River Basin, Jinan, Shandong 250100, China

See next page for additional authors

Custom Citation

NIU Geng, SHAO Long-tan, SUN De-an, WEI Chang-fu, GUO Xiao-xia, XU Hua, . Evolution law of pore-size distribution in soil-water retention test[J]. Rock and Soil Mechanics, 2020, 41(4): 1195-1202.

Evolution law of pore-size distribution in soil-water retention test

Authors

Geng NIU, Long-tan SHAO, De-an SUN, Chang-fu WEI, Xiao-xia GUO, and Hua XU

Rock and Soil Mechanics 2020 41(4): 1195−1202 ISSN 1000−7598
https: //doi.org/10.16285/j.rsm.2019.5785 rocksoilmech.researchcommons.org/journal

Evolution law of pore-size distribution in soil-water retention test

NIU Geng[1], SHAO Long-tan[1], SUN De-an[2, 3], WEI Chang-fu[3], GUO Xiao-xia[1], XU Hua[4]

1. State Key Laboratory of Structural Analysis of Industrial Equipment, Department of Engineering Mechanics, Dalian University of Technology, Dalian, Liaoning 116085, China

2. Department of Civil Engineering, Shanghai University, Shanghai 200444, China

3 Guangxi Key Laboratory of Geomechanics and Geotechnical Engineering, Guilin University of Technology, Guilin, Guangxi 541004, China

4. Shandong Province Administration of Haihe River Basin, Jinan, Shandong 250100, China

Abstract: This paper is to measure the soil-water retention curves (SWRC) of undisturbed and compacted soil specimens and compare the differences in measured data between these two soils. The mercury intrusion porosimetry (MIP) tests are conducted to explore the difference in the pore size distributions (PSD) between the undisturbed and compacted specimens and investigate the evolution law of PSD during drying. By considering shrinkage during drying, the basic parameters of SWRC can be determined based on the PSD. The results show that the undisturbed specimens in the wide suction range exhibit a unimodal PSD. The saturated compacted-specimen exhibits a unimodal PSD, but becomes the bimodal structure obviously during further drying. The SWRC of undisturbed specimens has a typical shape of "S", but the compacted specimens have a "horizontal stage" in the transition zone. The pore diameters governing the air entry value and residual value can be determined by the PSD of MIP tests, and then corresponding suctions can be calculated, which are consistent with the physical meaning.

Keywords: soil water retention curve; pore-size distribution; mercury intrusion porosimetry; air entry value; residual value

1 Introduction

The soil-water retention curve (SWRC) is used to express the relationship between the suction in the soil and the water content, and it is related to the permeability, strength and deformation. The SWRC also plays an important role in modeling the coupled hydro-mechanical behaviors of unsaturated soils[1]. Classical SWRC models are mostly based on macro-scale parameters. Due to the lack of micro-mechanism support, classical models show limitations, thus the study of the mechanical properties of unsaturated soil should not ignore the impact of micro-structure[2−3]. The microstructure of the soil plays a decisive role in governing the mechanical properties of all aspects. The mechanical properties of the soil can be understood in the macroscopic performance by linking to the microstructures. Therefore, to further understand the engineering properties of soil, a comprehensive study of the microstructure of the soil is required[4−5]. The water retention properties of soil are closely related to the pore structure. Within a certain range, the water-holding capacity of soil is a macroscopic expression of microscopic pore distribution[6−7]. Sun et al. discussed the evolution of the microstructure of the mud sample during drying process[8]. In recent years, nuclear magnetic resonance (NMR) technology has also been widely used to analyze the evolution of pores in soil and the distribution characteristics of pore water[9−10]. Simms et al. measured the pore distribution of soil under different suctions, and proposed the evolution law of pores during the dehydration process and brought it into the prediction of the water retention curve model[11]. Based on pore distribution, Hu et al. established a SWRC model considering soil deformation[12]. Tan et al. explained the effect of consolidation stress on the water retention curve based on pore size distribution (PSD) analysis[13]. Within a certain range, the characteristics of the pore structure play a decisive role in governing the property of the water retention curve, and the pore distribution of the soil can be used to explain the difference in water holding performance[7, 14]. Although scholars have made great progress in the study of water retention property, most of the above studies are aimed at soil samples with a single pore structure and explore the microstructure and water retention property under a single dry-wet cycle path. Nevertheless, studies comparing the evolution law of pore distribution in soil samples with different pore structures during the shrinking process are rarely reported, thus the relationship between pore distribution and water retention properties needs to be further investigated. Moreover, the theory to explain water retention properties from the perspective of pore distribution also needs to be further improved.

In this paper, the mercury intrusion test was used to measure the pore distribution of both undisturbed and reconstructed soil samples. The axis-translation method (ATM), filter paper method (FPM) and vapour equilibrium technique

Received: 30 April 2019 Revised: 5 July 2019
This work was supported by the National Natural Science Foundation of China (51479023, 11372078).
First author: NIU Geng, male, born in 1991, PhD candidate, majoring in unsaturated soil mechanics. E-mail: niugeng@mail.dlut.edu.cn

with saturated salt solution (VET) were employed to investigate the water retention behaviors. The pore distribution was used to explain the difference in macroscopic water holding characteristics. The air entry value (AEV) and residual values (RV) are also determined based on the pore distributions.

2 Unimodal and bimodal SWRCs and pore size distribution

2.1 Test materials and mercury intrusion porosimetry (MIP) test

The soil used in this study is fully weathered mudstone, taken from a slope in The Guangxi Zhuang Autonomous Region, China. Table 1 summarizes the physical and mechanical property indexes of this soil. The undisturbed samples and the compacted samples are used in this study, and the compacted samples were prepared with the same dry density as the undisturbed samples.

Mercury intrusion porosimetry (MIP) is currently the simplest and most effective way to measure pore volume and pore distribution of soil[16]. The principle of MIP is that the non-invasive liquid, mercury, will inflow into a void with the corresponding radius under the pressure during pressure increasing. Washburn's equation (Washburn, 1921), which is derived for capillary flow of a liquid in a cylindrical tube, is employed to calculate pore diameters based on the applied mercury pressures[7, 14, 16].

Table 1 Physical property values of completely weathered mudstone

Natural water conten /%	Maximum dry density /(g • cm^{-3})	Optimum water content /%	Liquid limit /%	Plastic limit /%	Plasticity index	Free swelling ratio /%	Natural dry density /(g • cm^{-3})	Natural void Ratio /%	Natural degree of saturation /%	Specific gravity
28.1	1.78	17	52.6	25.9	26.7	29.9	1.52	77	98.7	2.70

Undisturbed samples for MIP test were subjected to suction of 0.2, 2.3 and 38 MPa and compacted samples for MIP test were subjected to suction of 0, 2.3 and 38 MPa. All samples for MIP test were prepared by freeze drying. The MIP instrument is Micromeritics AutoPore IV with continuous pressurisation, which has a low-pressure range of 1.4–206 kPa and a high-pressure range of 138–413 640 kPa.

2.2 The evolution law of PSD of undisturbed samples during the drying process

Figure 1 gives the cumulative volumetric curves of the undisturbed samples under different suctions. It can be seen that all three curves have only one significant increase stage. The difference of the three curves reflects the shrinkage and deformation of the soil sample during the drying process. The final cumulative mercury intake represents the effective pore volume in the soil sample.

Figure 2 shows the pore volume distribution curves of undisturbed samples under different suctions, which reflects the proportion of pore volume of different pore sizes in the soil. It can be seen that the pore distributions of the undisturbed samples of fully weathered mudstone under different suctions are unimodal. In addition, the pore diameters of the three soil samples under different suctions are mainly distributed between 10 and 1 000 nm, and the peak pore diameter is about 100 nm. According to Zhang et al.'s criteria for distinguishing macro- and micro-pores[17], these PSDs of the undisturbed samples are mainly intra-aggregates or micro-pores. In a low suction range (0.2– 2.3 MPa), with the increase of suction, the PSD moves to the direction of the small pore (to the left), and the peak point decreases. The main reason is that in the range of high water content, the relatively large pores in the soil shrink preferentially, confirming with Tan et al.'s conclusion that the larger pores preferentially shrink during the drying process[18]. In the high suction range (2.3–38 MPa), with the increase of suction, the PSD moves to the direction of the large pore (to the right), and the peak point still decreases. The undisturbed sample has undergone multiple dry and wet cycles under natural conditions to produce unpredicted expansion and shrinkage deformations, thus there is a certain amount of tiny primary cracks in the soil. Under high suction, these tiny primary fissures develop as the PSD moves to the right[8]. However, the shrinkage of pores in the soil is greater than the amount of fissure development, and the soil sample still shows shrinkage on a macro level, and the peak of the PSD is still reduced.

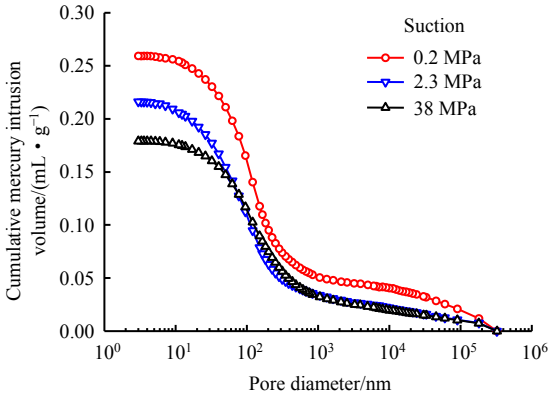

Fig.1 Cumulative intruded volume of undisturbed specimens under different suctions[15]

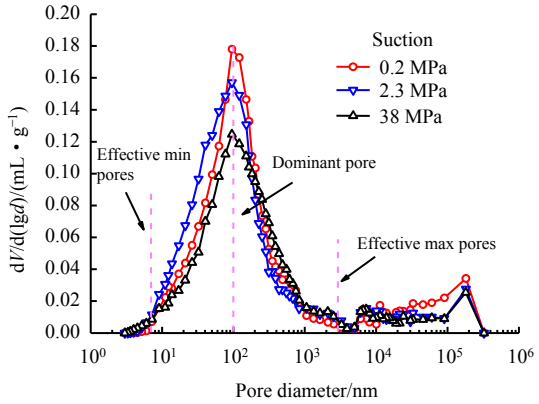

Fig.2 Pore-size distributions of undisturbed specimens under different maximum suctions

2.3 The evolution law of PSD of compacted samples during the drying process

Figure 3 presents the PSDs of compacted samples under different suctions. It can be seen that the saturated sample has a unimodal pore structure, which is mainly in a pore size range of 10 to 5000 nm, and the peak pore diameter is about 450 nm. The compacted sample at the suction of 2.3 MPa has a slightly bimodal pore structure, with two peaks in the range of 10 to 520 nm and 520 to 3 000 nm, respectively. When saturated soil sample dries to the suction of 2.3 MPa, the dominant pores are significantly reduced (peak value is reduced). With further drying (38 MPa), the dominant pores shrink further, forming a distinct bimodal pore structure. The sample with 38 MPa suction has two peaks, 11 to 300 nm and 300 to 2000 nm, respectively. At the same time, the relatively large pores shrink, showing the distribution curve moves toward the small pores within the relatively large pore range. According to the criteria for distinguishing macro- and micro-pores[17], there are mainly intra-aggregate pores and a small amount of inter-aggregate pores in the compacted sample. Compared with the undisturbed sample with the same dry density, the compacted sample has relatively large pores. Because the soil contains a small amount of free iron oxide, the ability of the soil to resist deformation is enhanced within a certain range. Therefore, the inter-aggregate pores do not shrink preferentially in the low suction range. However, under higher stress conditions, the inter-aggregate pores are relatively unstable. Due to the increase of the suction, the effective stress on the soil skeleton increases, causing relative sliding between the aggregates and then leading to shrinkage deformation of the relatively large pores[19].

2.4 Comparison of PSD between undisturbed and compacted samples

The undisturbed samples under 0.2, 2.3 and 38 MPa suction basically have a unimodal pore structure. The pore diameters of the dominant pores are about 100 nm, and the starting and ending pore diameters of the peak are about 9 and 2100 nm. Hu et al.[12] assumed that the pore distribution function after deformation can be obtained from the pore distribution function of reference state through translation and scaling. Figure 2 shows that as the suction increases, the pore structure of undisturbed soil is obviously scaled, while there is a slight translation. The undisturbed sample has undergone numerous dry and wet cycles under natural conditions, resulting in numerous expansion and shrinkage deformations, and the pores in the soil are relatively uniform and stable. In addition, in the shrinkage process, the basic shape of the pore distribution has not changed significantly[20].

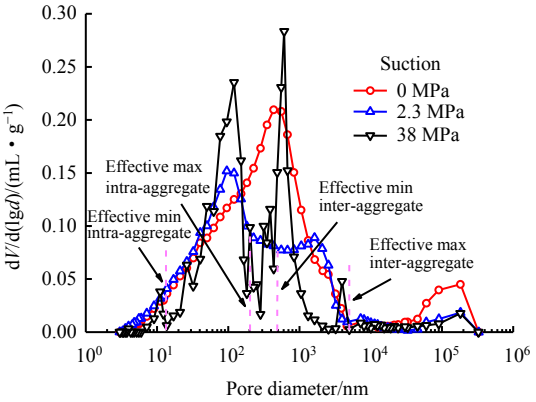

Fig.3 Pore-size distributions of undisturbed specimens under different maximum suctions

On the premise of the same void ratio as the undisturbed sample, the compacted sample also has unimodal pore structure in the saturated state. However, the pore diameter of the dominant pore is about 460 nm, and the peak is between 9 and 6000 nm, while there are some relatively larger pores in the compacted sample. For compacted sample, with the increase of suction (2.3 MPa), the dominant pores shrink, resulting in a bimodal pore structure. However, the inter-aggregates do not change significantly in this process. When the compacted soil subjected to a suction of 38 MPa, the sample exhibited a clear bimodal pore structure, and the relatively large pores also shrink. Therefore, the pore distribution function of the compacted sample in the higher suction state can not be obtained from the pore distribution curve of the saturated state through translation and scaling. Figures 2 and 3 indicate that under the same void ratio, there are relatively large inter-aggregate pores in the compacted sample than the undisturbed sample. Furthermore, for the compacted sample, the dominant pores shrink distinctly during water loss, and the inter-aggregate pores begin to shrink when the suction force reaches a high suction range.

3 SWRCs of undisturbed and compacted samples

The axis-translation method (ATM) [7], filter paper method (FPM) [21] and vapour equilibrium technique with saturated salt

solution (VET) [22] were employed to investigate the water retention behaviors of undisturbed and compacted soils. At the same time, the volumes are measured in this process.

Figure 4 shows the SWRC of the undisturbed sample in a wide suction range (drying process), and the curve is in S-type. According to the drawing method [6], the AEV is about 420 kPa, and the RV corresponds to the suction force of 26 MPa. Figure 5 shows the SWRC of the compacted sample in a wide suction range (drying process), which is a bimodal curve (a horizontal step appears in the transition section), confirming with Sun et al.[20]. According to the curve fitting[6], the AEV of inter-aggregates is about 73 kPa, and the RV of inter-aggregates is about 600 kPa. The AEV of intra-aggregate is about 2 100 kPa, and the RV of intra-aggregate is about 20 MPa.

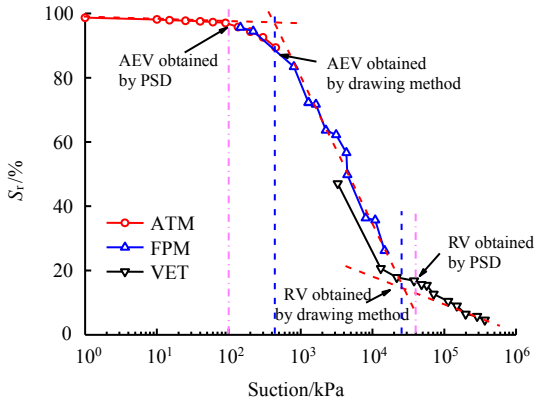

Fig.4 SWRC of undisturbed specimens in the full suction range

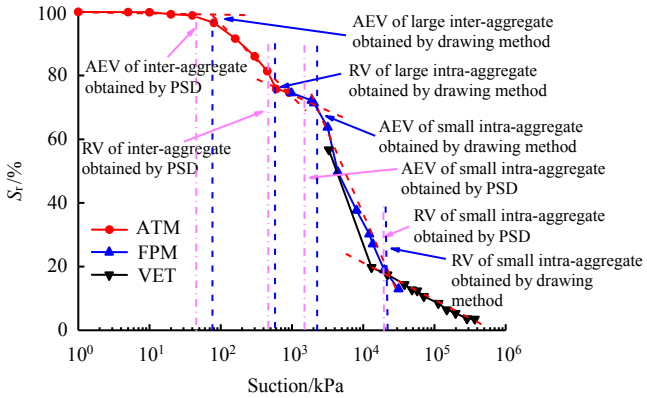

Fig.5 SWRC of compacted specimens in the full suction range

Figure 6 indicates that the SWRCs of the undisturbed and compacted samples of fully weathered mudstone have little difference. The SWRC of the compacted sample is slightly higher than that of the undisturbed sample in approximate saturation stage, due mainly to the rebound caused by the unloading of the compacted sample during the sample preparation process. In the low suction section (40−1 000 kPa), the SWRC of the intact sample is higher than that of the compacted sample The main reason is that the compacted sample has a certain amount of inter-aggregate pores, while the intact sample mainly possesses intra-aggregate pores. Therefore, according to the Young-Laplace equation, the water retention property of the compacted sample is relatively poorer in this stage. In the residual section, the water retention property of the two soil samples is basically the same.

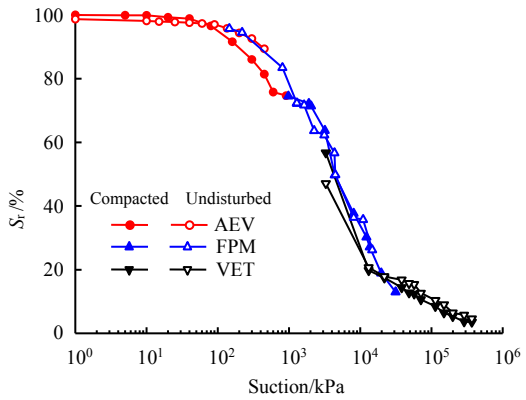

Fig.6 SWRCs of undisturbed and compacted specimens in the full suction range

4 Discussion on the relationship between SWRC and PSD

The undisturbed samples have a unimodal pore structure under a wide suction range, which is consistent with the classic inverted S-shape of SWRC of the undisturbed samples. The compacted samples under the suction of 2.3 and 38 MPa have a bimodal pore structure, which also explains the reason why the SWRC of the compacted samples appears as a step-shape in the transition section.

As shown in Fig.7, there is a corresponding relationship between pore size of the sample and the suction value according to the Young-Laplace equation. For MIP test, the relationship between applied external pressure and the corresponding pore diameter meets the Washburn equation:

$$p(d)=\frac{-4T_s\cos\theta}{d} \quad (1)$$

where $p(d)$ is the pressure applied in MIP（Pa）; d is the pore diameter (m); T_s is the mercury surface tensions (treated as 0.485 N/m); and θ is the mercury-soil contact angle (treated as 130°).

Therefore, the suction corresponding to a certain pore diameter in the soil has a certain relationship with the external pressure value corresponding to this same diameter in the MIP test[7, 17]:

$$s=0.196\times p(d) \quad (2)$$

where s is the suction.

The water retention property of soil is mainly controlled by

the pore size within a certain range, and the pore distribution is often used to explain the macroscopic water retention property[23]. When a certain suction is applied to the soil, there must be a pore with a defined pore diameter corresponding to this suction according to the capillary beam model and the Young-Laplace equation. Assuming that the water in the pores larger than this pore diameter is completely discharged, the pores smaller than this pore diameter are completely saturated[24, 25]. The intruded volume of mercury is equivalent to the water volume removed from the pores by the air intrusion for the same diameter of pores being intruded. In the MIP test, the point where mercury begins to invade the pores of the soil in large amounts corresponds to the AEV of the soil, and the point where mercury no longer invades the pores of the soil corresponds to the RV of the soil.

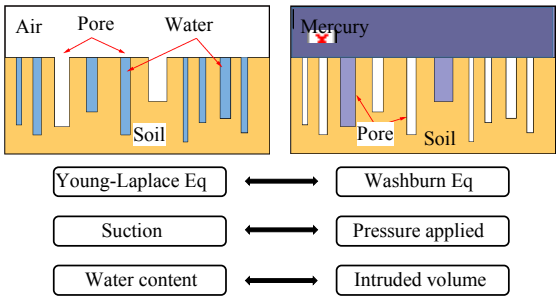

(a) Bundle of cylindrical capillaries (b) Conceptual sketch of MIP

Fig.7 Conceptual model of SWRC and mercury intrusion porosimetry method

According to the definition[6], the suction value corresponding to the air entering the soil is AEV of the soil. The suction corresponding to the point where the water in the soil is no longer obviously discharged with the increase of suction is the RV of the soil. The effective maximum pore represents the maximum pore in the soil that actually controls the air beginning to entry into soil. The suction value corresponding to the effective maximum diameter that can be calculated by Eq. (1) is the AEV. The effective maximum pore can be determined from the pore distribution function curve. The peak corresponding to the beginning of the peak shape (the direction of mercury intrusion) corresponds to the effective maximum pore. The effective minimum pore is the pore that actually controls the RV, and the corresponding suction can be calculated by Eq.(1). The pore corresponding to the peak point is the dominant pore, corresponding to the inversion point of the SWRC. The effective minimum pore can be determined from the pore distribution curve, and the ending point of the peak shape (the direction of mercury intrusion) is the effective minimum pore. For a unimodal SWRC, the starting point and ending point of the peak shape correspond to the effective maximum pore and the effective minimum pore, respectively, which controls the AEV and RV in SWRC, as shown in Fig. 8.

For the soil with bimodal pore structure, the SWRC is controlled by both the inter-aggregate and intra-aggregate pores. The water retention curve has have two descending sections with different slopes and a horizontal section in the transition zone. Therefore, the bimodal SWRC contains 4 key points: the AEV of inter-aggregates, the RV of inter-aggregates, the AEV of intra-aggregates and the RV of intra-aggregates[23]. For pore distribution density curve, relatively large peak is controlled by the inter-aggregate pores, and relatively small peak is controlled by the intra-aggregate pores. As shown in Fig.9, the effective maximum inter-aggregate pores control the first AEV, and the effective minimum inter-aggregate pores control the first RV. The effective maximum intra-aggregate pores control the second AEV, and the effective minimum intra-aggregate pores control the second RV. The pores corresponding to the two peak points are the dominant pores of inter-aggregate and intra-aggregate, which correspond to the inversion points of the two descending sections of the SWRC, respectively. The pore diameter which controls the AEV and RV can be determined from the pore distribution density curve. The starting and ending points (slope abrupt change point) of the first peak shape (macro-pores) correspond to the effective maximum and minimum inter-aggregate pores, respectively. The starting and ending points (slope abrupt change point) of the second peak shape (micro-pore) correspond to the effective maximum and minimum intra-aggregate pores, respectively.

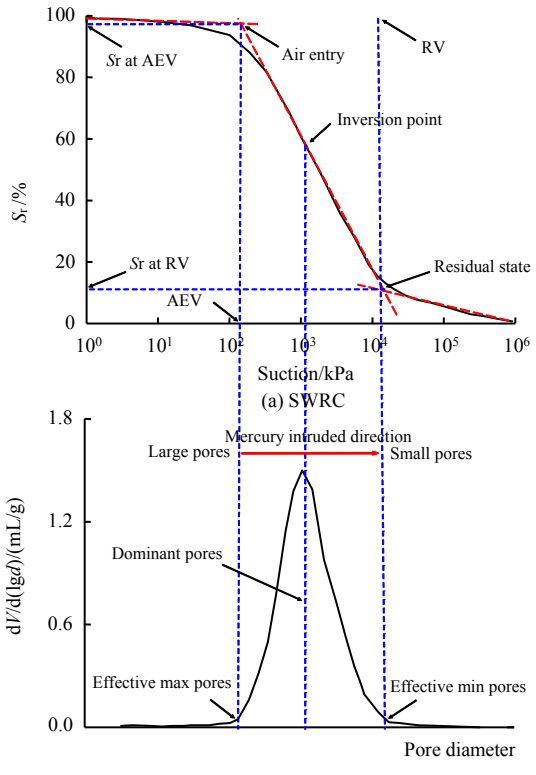

(b) PSD

Fig.8 Conceptual model of unimodal SWRC and mercury intrusion porosimetry model

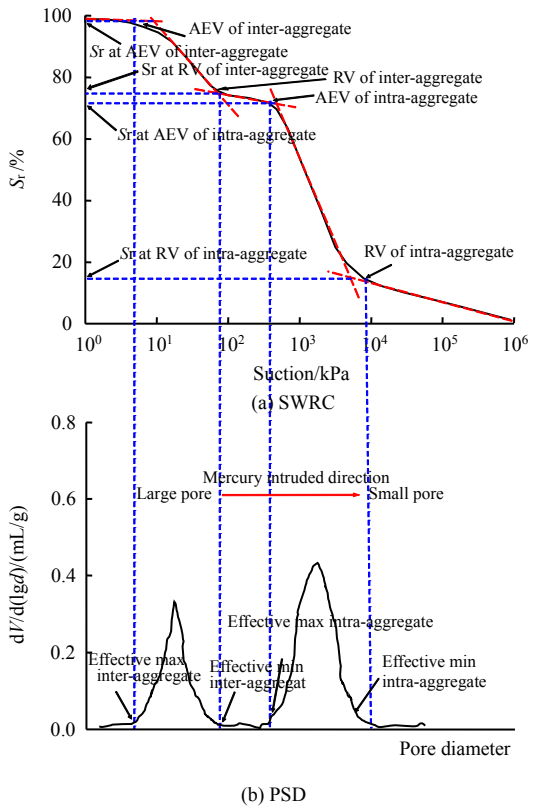

Fig.9 Conceptual model of bimodal SWRC and mercury intrusion porosimetry model

5 Determination of basic parameters of SWRC based on PSD

At present, the determination of the basic parameters of SWRC is mainly based on making a tangent line on the measurement data (drawing method)[6]. The AEV is estimated according to the intersection point of the tangent line between the boundary and the transitional section, and the RV is estimated according to the intersection point of the tangent line between the transition section and the residual section. The traditional method for estimating the SWRC parameters has subjective assumptions, and must be based on measurement data of SWRC in the full suction range[26].

Table 2 Basic parameters of unimodal SWRC by PSDs

Suction /kPa	Effective max diameter /nm	Corresponding pressure applied /kPa	Corresponding suction /kPa	Effective min diameter /nm	Corresponding pressure applied /kPa	Corresponding Suction /MPa
0	2 500	496	95	–	–	–
38	–	–	–	7	172 413	33

As shown in Fig.4, according to the traditional method, the AEV of undisturbed sample is about 430 kPa, and the suction corresponding to the RV is about 27 MPa. It can be estimated from Figure 2 that the pore diameter which controls the AEV is about 2500 nm, and the RV can be calculated according to Eq. (2) to be 95 kPa. While suction increasing, the soil will shrink and deform[27]. Since the RV is generally in the range of high suction, the PSD curve under high suction should be used when estimating the pore size that controls RV. Using the PSD curve at a suction of 38 MPa, we can determine the pore diameter governing the RV is about 7 nm, and the corresponding suction is 33 MPa. The basic parameters of the unimodal SWRC determined by the PSD curve are shown in Table 2. As can be seen in Fig. 4, the AEV and RV determined by the PSD are different from the values obtained by traditional determination method. However, according to the definition of the AEV, the AEV determined by the pore distribution is more reasonable. The degree of saturation corresponding to the AEV determined by the tangent line method is below 90%, which is unreasonable. If this value is employed in the constitutive model, it will cause the prediction error of the suction which will be too high in the near saturation state. The AEV point determined by the PSD is basically located near the separation point between the tangent of the boundary segment and the measurement data, which also has physical meaning. The RV point determined by the drawing method and the point obtained based on the PSD show little difference, and are basically considered to be consistent.

Table 3 Basic parameters of bimodal SWRC obtained by PSDs

Suction /kPa	Effective max inter-aggregate pore /nm	Corresponding pressure applied /kPa	Suction /kPa	Effective max intra-aggregate pore /nm	Corresponding pressure applied /kPa	Suction /kPa
0.0	5 000	248	48	–	–	–
2.3	200	6 137	1 200	500	2 482	490
38	–	–	–	11	151 724	22 000

Based on the traditional drawing method, it can be seen from Fig. 5 that, the AEV of the inter-aggregate pores for compacted sample is about 70 kPa, and the RV of the inter-aggregate pores is about 600 kPa. The AEV of the intra-aggregate pores for compacted sample is 2100 kPa, and the RV of the intra-aggregate pores is 20 MPa. Based on the PSD curve under the suction of 0.2 MPa, it can be seen from Fig. 3 that the effective maximum pore diameter of the inter-aggregates is about 5000 nm. According to Eq. (2), this pore controls the AEV, and the corresponding suction can be calculated which is 48 kPa. According to the pore distribution curve under the suction of 2.3 MPa, the effective minimum diameter of the inter-aggregate pores is about 5000 nm. This pore controls the RV of the inter-aggregates, and the corresponding suction is 490 kPa determined by Eq. (2). Using the pore distribution curve under suction of 2.3 MPa, we can

determine the effective maximum diameter of the intra-aggregate pores is about 200 nm. This type of pore governs the AEV of the intra-aggregates, and the corresponding suction is 1200 kPa calculated by Eq. (2). According to the pore distribution curve under the suction of 38 MPa, the effective minimum diameter of the intra-aggregate pores is about 11 nm. This type of pore governs the RV of the intra-aggregates, and the corresponding suction of intra-aggregates is 22 MPa determined by Eq. (2). The basic parameters of the bimodal SWRC determined by the pore distribution curve are shown in Table 3. The AEV is defined as the suction value corresponding to the gas entering the saturated soil and the RV is defined as the point where the capillary water content in the soil does not change significantly with increasing suction. It can be seen from Figs. 4 and 5 that the AEV and RV based on the PSD obtained from the MIP test are more reasonable.

6 Conclusions

The SWRCs of undisturbed and reconstituted samples of completely weathered mudstone are measured and the differences of two soils are investigated. The MIP tests are used to explore the difference in the PSD between undisturbed and compacted specimens and investigate the evolution law of the PSD during drying. Considering shrinkage during drying, the basic parameters of SWRC can be determined based on the PSD. The following conclusions can be obtained from this study:

The undisturbed sample basically has a unimodal pore structure in a wide suction range, and the pore distribution curve under a high suction can be obtained by scaling and translation of the PSD under a low suction. The saturated compacted sample has the unimodal pore structure. However, with the increase of suction, there is a tendency for compacted sample to exhibit a bimodal pore structure. The compacted sample at 38 MPa suction shows an obvious bimodal pore structure. Therefore, the pore distribution curve under the high suction cannot be obtained by scaling and translation of the PSD under the low suction of compacted samples.

The SWRC of the undisturbed sample is a classic “inverted S” shape, while the SWRC of the compacted sample has a horizontal step in the transitional section. In a low suction range, the SWRC of the compacted sample is lower than that of the undisturbed sample. This is mainly because there are some relatively large inter-aggregate pores in the compacted sample. In the high suction range, the SWRC of undisturbed sample and the compacted sample are basically the same. The undisturbed samples all have unimodal pore structures, while the compacted samples under higher suction have a bimodal pore structure, which also explains the difference in the shape of the SWRCs of the two soil samples.

Based on the PSD curve, the pore sizes that control the AEV and RV are determined, and the corresponding suction value can be calculated. The soil sample shrinks and deforms during the drying process. Therefore, the pore size controlling the AEV is obtained from the PSD curve under a relatively low suction, while the pore size controlling the RV is obtained from the PSD curve under a relatively high suction. Compared with the basic parameters of the SWRC determined by the traditional drawing method, the AEV and the RV determined by the PSD curve have more reasonable physical meaning.

References

[1] LU N, LIKOS W J. Unsaturated soil mechanics[M]. [S. l.]: Wiley, 2004.

[2] CAI Guo-qing, WANG Ya-nan, ZHOU An-nan, et al. A microstructure-dependent hydro-mechanical coupled constitutive model for unsaturated soils[J]. Chinese Journal of Geotechnical Engineering, 2018, 40(4): 618−624.

[3] XU Y. Calculation of unsaturated hydraulic conductivity using a fractal model for the pore-size distribution[J]. Computers and Geotechnics, 2004, 31(7): 549−557.

[4] JIANG Ming-jing. New paradigm for modern soil mechanics: geomechanics from micro to macro[J]. Chinese Journal of Geotechnical Engineering, 2019, 41(2): 195−254.

[5] CHEN Zheng-han, GUO Nan. New developments of mechanics and application for unsaturated soils and special soils[J]. Rock and Soil Mechanics, 2019, 40(1): 1−54.

[6] FREDLUND D G, XING A. Equations for the soil-water characteristic curve[J]. Canadian Geotechnical Journal, 1994, 31(3): 521−532.

[7] NIU Geng, SUN De-an, WEI Chang-fu, et al. Water retention curve of complete-intense weathering mudstone and its estimation from pore-size distribution[J]. Rock and Soil Mechanics, 2018, 39(4): 1337−1345.

[8] SUN W J, CUI Y J. Investigating the microstructure changes for silty soil during drying[J]. Géotechnique, 2017, 68(4): 370−373.

[9] LU Hai-feng, CHEN Pan, WEI Chang-fu. Evolution of suction strength of clayed soil under drying conditions and its microscopic mechanism[J]. Rock and Soil Mechanics, 2017, 38(Suppl.2): 145−150.

[10] TIAN Hui-hui, WEI Chang-fu, WEI Hou-zhen, et al. A NMR-based analysis of drying processes of compacted clayed sands[J]. Rock and Soil Mechanics, 2014, 35(8): 2129−2136.

[11] SIMMS P H, YANFUL E K. Measurement and estimation of pore shrinkage and pore distribution in a clayey till during soil-water characteristic curve tests[J]. Canadian Geotechnical Journal, 2001, 38(4): 741−754.

[12] HU Ran, CHEN Yi-feng, ZHOU Chuang-bing. A water retention curve model for deformable soils based on pore size[J]. Chinese Journal of Geotechnical Engineering, 2013, 35(8): 1451−1462.

[13] TAN Yun-zhi, HU Xin-jiang, YU Bo, et al. Water retention properties and mesomechanism of silt under consolidation effect[J]. Rock and Soil Mechanics, 2013, 34(11): 3077−3084.

[14] ROMERO E, GENS A, LLORET A. Water permeability, water retention and microstructure of unsaturated compacted Boom clay[J]. Engineering Geology, 1999, 54(1-2): 117−127.

[15] NIU G, SUN D, SHAO L, et al. The water retention behaviours and pore size distributions of undisturbed and remoulded complete-intense weathering mudstone[J]. European Journal of Environmental and Civil Engineering, 2019: 1-18. DOI: 10.1080/19648189. 2019.1572544.

[16] SASANIAN S, NEWSON T A. Use of mercury intrusion porosimetry for microstructural investigation of reconstituted clays at high water contents[J]. Engineering Geology, 2013, 158: 15−22.

[17] ZHANG F, CUI Y J, YE W M. Distinguishing macro-and micro-pores for materials with different pore populations[J]. Géotechnique Letters, 2018, 8(2): 102−110.

[18] TAN Yun-zhi, YUN Bo, LIU Xiao-ling, et al. Pore size evolution of compacted laterite under desiccation shrinkage process effects[J]. Rock and Soil Mechanics, 2010, 31(5): 1427−1430.

[19] BURTON G J, SHENG D, CAMPBELL C. Bimodal pore size distribution of a high-plasticity compacted clay[J]. Geotechnique Letters, 2014(4): 88−93.

[20] SUN D, YOU G, ANNAN Z, et al. Soil-water retention curves and microstructures of undisturbed and compacted Guilin lateritic clay[J]. Bulletin of Engineering Geology and the Environment, 2016, 75(2): 781−791.

[21] LEONG E C, HE L, RAHARDJO H. Factors affecting the filter paper method for total and matric suction measurements[J]. Geotechnical Testing Journal, 2002, 25(3): 1−12.

[22] DELAGE P, AUDIGUIER M, CUI Y J, et al. Microstructure of a compacted silt[J]. Canadian Geotechnical Journal, 1996, 33(1): 150−158.

[23] SIMMS P H, YANFUL E K. A pore-network model for hydromechanical coupling in unsaturated compacted clayey soils[J]. Canadian Geotechnical Journal, 2005, 42(2): 499−514.

[24] OR D, TULLER M. Cavitation during desaturation of porous media under tension[J]. Water Resources Research, 2002, 38(5): 19-1-19-14.

[25] LI X, LI J H, ZHANG L M. Predicting bimodal soil-water characteristic curves and permeability functions using physically based parameters[J]. Computers and Geotechnics, 2014, 57: 85−96.

[26] ZHAI Q, RAHARDJO H. Determination of soil-water characteristic curve variables[J]. Computers and Geotechnics, 2012, 42: 37−43.

[27] HUANG Qi-di, CAI Guo-qing, ZHAO Cheng-gang. Microstructure evolution of unsaturated soil during drying process[J]. Rock and Soil Mechanics, 2017, 38(1): 165−173.